Use of High-Order Sensitivity Analysis and Reduced-Form Modeling to Quantify Uncertainty in Particulate Matter Simulations in the Presence of Uncertain Emissions Rates: A Case Study in Houston

Wenxian Zhang*, Marcus A. Trial, Yongtao Hu, Athanasios Nenes, Armistead G. Russell

*Corresponding author. Telephone: 1-404-825-0960, Email address: wzhang@trinityconsultants.com

Abstract

Regional air quality models are widely used to evaluate control strategy effectiveness. As such, it is important to understand the accuracy of model simulations to establish confidence in model performance and to guide further model development. Particulate matter with aerodynamic diameter less than 2.5 micrometers ($PM_{2.5}$) is regulated as one of the criteria pollutants by the National Ambient Air Quality Standards (NAAQS), and $PM_{2.5}$ concentrations have a complex dependence on the emissions of a number of precursors, including SO_2, NO_x, NH_3, VOCs, and primary particulate matter (PM). This study quantifies how the emission-associated uncertainties affect modeled $PM_{2.5}$ concentrations and sensitivities using a reduced-form approach. This approach is computationally efficient compared to the traditional Monte Carlo simulation. The reduced-form model represents the concentration-emission response and is constructed using first- and second-order sensitivities obtained from a single CMAQ/HDDM-PM simulation. A case study is conducted in the Houston-Galveston-Brazoria (HGB) area. The uncertainty of modeled, daily average $PM_{2.5}$ concentrations due to uncertain emissions is estimated to fall between 42% to 52% for different simulated concentration levels, and the

uncertainty is evenly distributed in the modeling domain. Emission-associated uncertainty can account for much of the difference between simulation and ground measurements as 60% of observed $PM_{2.5}$ concentrations fall within the range of one standard deviation of corresponding simulated $PM_{2.5}$ concentrations. Uncertainties in meteorological fields as well as the model representation of secondary organic aerosol formation are the other two key contributors to the uncertainty of modeled $PM_{2.5}$. This study also investigates the uncertainties of the simulated first-order sensitivities, and found that the larger the first-order sensitivity, the lower its uncertainty associated with emissions. Sensitivity of $PM_{2.5}$ to primary PM has the lowest uncertainty while sensitivity of $PM_{2.5}$ to VOC has the highest uncertainty associated with emission inputs.

1. Introduction

Significant effort has been expended to improve air quality due to its influence on human health and the environment. The United States Environmental Protection Agency (U.S. EPA) sets National Ambient Air Quality Standards (NAAQS) to protect public health and the environment. Particulate matter (PM), including fine particles with 2.5 micrometers in diameter and smaller ($PM_{2.5}$), is currently regulated as one of the NAAQS criteria pollutants. The harmful effects of PM on human health have been a focus as exposure to $PM_{2.5}$ is associated with respiratory and cardiovascular disease (Zanobetti et al., 2000; Schwartz, 1994, Dockery et al., 1993). A recent study (Kaiser, 2005) found that fine particles are potentially of more concern than larger particles in causing respiratory disease and premature death due to their ability to penetrate deep into the lung. In order to more effectively protect the public from adverse health effects due to exposure to fine particles, in December 2012, U.S. EPA tightened the primary

NAAQS for the annual average concentration of fine particles from 15 μg m^{-3} to 12 μg m^{-3}. Their contribution to acidic deposition and visibility are also concerns (e.g., Galloway et al., 2004; Watson 2002).

PM control is perhaps the most complex aspect of current air quality management. The complexity comes from the many components of PM and formation routes. Regional air quality models are frequently used in air quality management to evaluate the effectiveness of emissions control (U.S. EPA, 2004). The accuracy of these models is limited by their representation of the complex chemical and physical processes of pollutant transport and transformation, as well as the lack of accuracy in inputs (e.g., emissions rates, meteorological conditions, and initial and boundary conditions). Previous studies have investigated model uncertainties on ozone, focusing on uncertainties due to emission estimates, initial and boundary conditions, grid size, and chemical reactions (e.g., Hanna. et al., 2001, 1998; Cohan et al., 2010; Pinder et al., 2009). Uncertainties in emission inventories remain a leading cause for discrepancies between models and observations (Xiao et al., 2010). As such, quantification of the influence of uncertain emission inventories on simulated concentrations of $PM_{2.5}$ is informative to the air quality management processes as well as to guide model improvement, and the importance of that information is becoming more apparent as an increased focus is placed on $PM_{2.5}$. Of further importance is the uncertainty in capturing the response of air quality models to emission changes, i.e., the uncertainty of the sensitivity of air quality models to emission changes.

Estimates of the uncertainty of air quality model prediction from uncertainties in input parameters has relied heavily on Monte Carlo simulations that randomly sample model inputs (according to their probability distributions) and then quantified the uncertainties of model outputs (e.g. pollutant concentrations and sensitivities) by using the ensemble outputs obtained

from the Monte Carlo simulations (e.g., Tian et al., 2010; Pinder et al., 2009; Hanna et al., 1998, 2001). Initially, studies conducted the Monte Carlo simulations by running the underlying air quality model multiple times (e.g., Deguillaume et al., 2008; Hanna et al., 1998 and 2001; Bergin et al., 1999). However, this approach becomes computationally expensive and cumbersome for three-dimensional time-dependent models applied over large domains. More recently, studies have employed a reduced form model (RFM) approach, which substantially reduces the computational cost (e.g. Kerl et al., 2014; Napenelok et al., 2011; Tian et al., 2010; Digar and Cohan, 2010; Pinder et al., 2009). This approach constructs a reduced form model of the underlying air quality model by capturing concentration-parameter responses of the original model. High order direct sensitivity analysis is efficient at extracting the concentration-parameter response by simultaneously providing first- and second-order sensitivity coefficients along with the base concentration simulation. This advanced sensitivity technique has been implemented in air quality models (e.g., the Community Multiscale Air Quality (CMAQ) model (Byun and Schere, 2006) for gas and aerosol species (Zhang et al., 2012; Napenelok et al., 2011; Hakami et al., 2003; Yang et al., 2007), and the Comprehensive Air Quality Model with Extensions (CAMx) (ENVIRON, 2005; Cohan et al., 2010) for gas and aerosol species). It has already been applied to characterize the uncertainty of modeled ozone production (Napenelok et al., 2011; Tian et al., 2010; Digar and Cohan, 2010; Pinder et al., 2009) and to investigate the influence of reaction constants' uncertainties on ozone sensitivities (Xiao et al., 2010; Cohan et al., 2010).

This paper discusses application of the RFM based on CMAQ to efficiently quantify the emission-associated uncertainties of the simulated $PM_{2.5}$ concentrations and sensitivities for an air pollution episode in the Houston region. An underestimation of VOC emissions in the Houston Ship Channel (HSC) has been found by a number of studies (e.g. Kim et al., 2011,

Cowling et al., 2007, and Ryerson et al., 2003), and Kim et al. (2011) found an overestimation of NO_x emissions over the HSC in the 2005 National Emissions Inventory (NEI). The complex concentration-emissions responses due to emissions from the petrochemical plants and the unique geographic and meteorological conditions makes this area a good case for studying the emission uncertainty. Using high-order sensitivity analysis, this paper evaluated the impact of uncertain emission inventories on $PM_{2.5}$ concentrations and sensitivities.

2. Methods

2.1 Modeling system

Air quality modeling is conducted using CMAQ (Byun and Schere, 2006) version 4.7.1 (CMAQ v4.7.1) with the SAPRC 99 (Carter, 2000) chemical mechanism and the AERO5 aerosol module (Foley et al., 2010; Carlton et al., 2010). CMAQ v4.7.1 has been equipped with the Decoupled Direct Method in Three Dimensions (DDM-3D) (Napelenok et al., 2006), which has been extended to high-order DDM-3D for particulate matter (HDDM-3D/PM) by Zhang et al. (2012), and it was the latest version of CMAQ that had HDDM-3D/PM implemented in when this work was carried out.

The CMAQ model application here uses three one-way nested modeling domains (Figure S1). The outer-most domain covers the entire continental United States and portions of Canada and Mexico with 36- by 36-km horizontal grids; the middle domain covers eastern Texas and the surrounding states of Oklahoma, Arkansas, and Louisiana with 12- by 12- km grids; the inner-most domain covers southeastern Texas which contains the Houston-Galveston-Brazoria (HGB) region where intense emissions from petrochemical industries occur. The three domains have 13 vertical layers extending approximately 16 km above ground, with seven layers below 1 km.

The Weather Research and Forecasting (WRF) model is widely used in atmospheric research and weather forecasting. This application used the WRF model to prepare the meteorological fields and is run with 34 layers using four-dimensional data assimilation (FDDA) techniques and the Noah land-surface model with MODIS landuse data. The Sparse Matrix Operator Kernel for Emissions (SMOKE) is used to process emissions to provide gridded, CMAQ-ready emissions. The inventory used is the U.S. National Emissions Inventory (NEI) of 2005 (ftp://ftp.epa.gov/EmisInventory/2005v4/) (Figure 1).

2.2 Reduced-form model of CMAQ

Uncertainty analysis performed here is based on a RFM of CMAQ. The RFM represents the relationship between pollutant concentrations and the model inputs in a straightforward way and can be used to efficiently propagate uncertainties from model inputs to outputs. Constructing the RFM involves Taylor series expansion of the pollutant concentration at a given time and location for fractional perturbations in sensitivity parameters of interest (Eq. 1) (e.g., Cohan et al. 2005). The sensitivity parameters can be emissions rates, chemical reaction rates, or initial and boundary conditions. Only emissions rates are considered here for studying the emission-associated model uncertainties:

$$C_i^* = C_{i,0} + \sum_{j=1}^{J} \Delta\varepsilon_j S_{i,j}^{(1)} + \frac{1}{2}\sum_{j=1}^{J} \Delta\varepsilon_j^2 S_{i,j,j}^{(2)} + \sum_{j\neq k} \Delta\varepsilon_j \Delta\varepsilon_k S_{i,j,k}^{(2)} + H.O.T. \quad (1)$$

where C_i^* and $C_{i,0}$ denote the concentration of pollutant i with and without perturbations in sensitivity parameters, respectively. $S_{i,j}^{(1)}$, $S_{i,j,j}^{(2)}$, and $S_{i,j,k}^{(2)}$ are semi-normalized sensitivity coefficients. *i* denotes the i^{th} species, *j* and *k* denotes the j^{th} and k^{th} emissions rates. Note that C_i^*, $C_{i,0}$, $S_{i,j}^{(1)}$, $S_{i,j,j}^{(2)}$, and $S_{i,j,k}^{(2)}$ all vary with time and location, and the notations for time and

location are omitted for brevity. $\Delta\varepsilon_j$ is the relative change (e.g., 0 is no change and 1 is a 100% increase) in the j^{th} emission rate. There is considerable flexibility in how the j^{th} emission rate is specified: j can be the emissions of a specific species from all sources, the emissions of all species from a specific source, the emissions of multiple pollutants from a specific location, or various combinations. In this study, we consider the five major groups of emitted species, sulfur dioxide (SO_2), nitrogen oxides (NO_x), volatile organic compounds (VOCs), ammonia (NH_3), and primary PM, that impact $PM_{2.5}$ concentration. *H.O.T.* stands for higher order terms.

CMAQ-HDDM-3D is used to calculate local first- and second-order semi-normalized sensitivity coefficients. This sensitivity technique is efficient as it simultaneously computes all sensitivity coefficients along with concentrations in one model run. The controlling equations for sensitivity coefficients are derived by differentiating governing equations for the concentrations with respect to the sensitivity parameters (Dunker 1981). Thus, equations involving sensitivities and concentrations have a similar structure and are calculated using the same numerical algorithms. First- and second-order sensitivity coefficients calculated by CMAQ-HDDM-3D have been evaluated by comparing them with traditional finite differences and good agreement has been observed for both gas-phase species and particulate matter (Zhang et al., 2012; Hakami et al., 2003). Extensive evaluation of the CMAQ-HDDM/PM sensitivities and the RFM used in this study has been conducted, and demonstrated the reliability of the RFM performance in replicating the results of the original CMAQ (Figures S3-S5).

The RFM for first order sensitivities can be constructed based on second-order sensitivities (e.g., Tian et al., 2010; Cohan et al. 2005). The formulation of the RFM is similar to that of the concentrations:

$$S_{i,j}^{(1)*} = S_{i,j,0}^{(1)} + \Delta\varepsilon_j S_{i,j,j}^{(2)} + \sum_k \Delta\varepsilon_k S_{i,j,k}^{(2)} + H.O.T., \quad (2)$$

where $S_{i,j}^{(1)*}$ and $S_{i,j,0}^{(1)}$ respectively denote first order sensitivity of pollutant *i* to emission rate *j* with and without considering the uncertainty in the emissions rates. $S_{i,j,j}^{(2)}$ is second-order self sensitivity of pollutant *i* to emissions rates *j*. $S_{i,j,k}^{(2)}$ is second-order cross sensitivity of pollutant *i* to emissions *j* and *k*. $\Delta\varepsilon_j$ is the relative emission change as described for Eq. 1. An evaluation of Eq. 2 using the sensitivity output from the original CMAQ-HDDM shows an excellent agreement between the two (Figure S6).

2.3 Quantification of emission-associated uncertainties

Monte Carlo simulations using the reduced-form CMAQ are applied to quantify the emission-associated uncertainties of modeled $PM_{2.5}$ concentrations and sensitivities. Three steps are involved in the Monte Carlo simulations. The first step is to sample the emissions rates of interest based on their relative uncertainties and probability distributions. The second step is to propagate uncertainties through the reduced-form model and collect an ensemble of model outputs. The third step is to quantify model uncertainties from the output ensemble.

Emissions rate uncertainties are assumed to be log-normally distributed, as is approximately found for many environmental geographical variables that are constrained to be positive (Hanna et al., 1998). This study focuses on the domain-wide total (anthropoengic+biogenic) emissions of five major pollutants that impact atmospheric PM levels: SO_2, NO_x, VOC, NH_3, and primary PM. As uncertainties explicit to NEI 2005 are unavailable, the uncertainties of these emissions are obtained from previous studies, which may not be exactly the same as the uncertainties in 2005 NEI but provide good references for estimating the uncertainties in 2005 NEI. Hanna et al. (2001) summarized the estimates of uncertainty factors for NO_x and VOC emissions from major point, mobile, biogenic, and area sources. The

NARSTO PM assessment (2004) provides the uncertainties in the national emission inventory for SO_2, NO_x, VOC, NH_3, and primary PM from various source categories. Combining the confidence levels in the NARSTO assessment with the uncertainty factors in Hanna et al. (2001), the uncertainty factors of the emissions rates of the five pollutants of interest can be estimated (Table 1).

A random number generator is applied to produce multiple sets of input emissions rates given their probability distributions and uncertainties. This study selected a sampling size of 1000, which has been demonstrated to achieve sufficient convergence in the uncertainty analysis on ozone simulation conducted by Pinder et al. (2009). Each sample includes a separate value for each emitted species.

For every grid cell and time step, the multiple sets of sampled emissions rates were input to the RFM and generate 1000 values of $PM_{2.5}$ concentrations, from which the relative uncertainty is calibrated. Among various methods to calibrate the relative uncertainty, we selected the method used by Tian et al. (2010). They calculated the relative uncertainty of simulated $PM_{2.5}$ at each grid cell by dividing a half of the 68.3% confidence interval (CI) (corresponding to 2 standard deviations) of the 1000 values by their median (Eq. 3) to exclude potential outliers due to accumulating predictive uncertainties of the RFM at extreme emission changes. The standard deviation (SD) of the simulated $PM_{2.5}$ at each grid is equal to the product of the relative uncertainty and the median (Eq. 4).

$$Relative\ Uncertainty = \frac{68.3\%CI}{2 \times median} = \frac{84.15^{th}\ percentile - 15.85^{th}\ percentile}{2 \times median} \quad (3)$$

$$Standard\ Deviation = \frac{68.3\%CI}{2} = \frac{84.15^{th}\ percentile - 15.85^{th}\ percentile}{2} \quad (4)$$

The method used to calculate sensitivities (sensitivities to domain wide emission changes applied over the duration of the simulation) and the method used to calculate uncertainties impact interpretation of the results. Calculation of uncertainties assumes that emission errors are the same across space and time for each pollutant, but the errors in emissions between species is independent. Thus, the actual uncertainties are likely less (much of the uncertainties in the emissions are likely due to local (time and space) variations in the emissions), but can be underestimates in that some of the emission uncertainties can be correlated between species (e.g., due to uncertainties in activities in a specific source that emits more than one species). We have chosen to use the approach most common in prior studies.

3. Results and Discussion

3.1 Model evaluation

Surface meteorological fields simulated by WRF are evaluated by using hourly surface observations in the U. S. and Canada. The bias and root mean square errors (RMSE) for the three domains are well within the range considered to be acceptable for air quality modeling (Table 2) (Emery et al., 2001; Hanna and Yang, 2001). Good agreement between the WRF simulation and observations minimizes uncertainty due to input meteorological fields.

CMAQ performance is evaluated using data retrieved from the Air Quality System (AQS; available at http://www.epa.gov/ttn/airs/airsaqs/detaildata/downloadaqsdata.htm). Simulated 8-hr averaged ozone and daily averaged $PM_{2.5}$ concentrations are compared with monitoring data inside the 4 km domain. The mean normalized bias (MNB) and mean normalized error (MNE) for 8-hr averaged ozone are -7 ppb and 19%, respectively, well within suggested performance levels (EPA 2007) (Table S1). The definition of MNB and MNE is shown by Eqs. 5 and 6, where C_m and C_o are the modeled and observed $PM_{2.5}$ concentrations, respectively. $PM_{2.5}$

simulations are commonly evaluated by using mean fractional bias (MFB) and mean fractional error (MFE) (see Eqs 7, 8, and Fig. 2). For this simulation, MFB and MFE are -30% and 54%, respectively, which are within the acceptable range according to the guidance of EPA (2007). The MFBs of daily averages of sulfate, nitrate, ammonium, organic carbon (OC), and EC are -65%, -122%, -59%, -25%, and 47%, respectively. Graphically, these MFBs and MFEs are shown and compared against suggested criteria using bugle plots (Boylan and Russell, 2006) (Figure 2). CMAQ performance of $PM_{2.5}$ is further detailed in Table S1. Nitrate aerosols have higher MFB and MFE than other $PM_{2.5}$ species. This is largely due to the limitation of the model in representing the complex processes involved in nitrate aerosol formation (e.g., Kwok et al. 2013, Civerolo et al., 2010, Zhang et al., 2009, Yu et al., 2005).

$$MNB = \frac{1}{N}\sum_{i=1}^{N}\frac{C_m - C_o}{C_o} \quad (5)$$

$$MNE = \frac{1}{N}\sum_{i=1}^{N}\left|\frac{C_m - C_o}{C_o}\right| \quad (6)$$

$$MFB = \frac{2}{N}\sum_{i=1}^{N}\frac{C_m - C_o}{C_m + C_o} \quad (7)$$

$$MFE = \frac{2}{N}\sum_{i=1}^{N}\left|\frac{C_m - C_o}{C_m + C_o}\right| \quad (8)$$

3.2 Uncertainty of modeled concentrations

Using the sampling results to drive the reduced-form CMAQ gives an ensemble of pollutant concentrations for each grid cell at every hour. In this study, daily averages of $PM_{2.5}$ concentrations are studied because that is one metric used in the NAAQS, and it is commonly used for model performance evaluation. Since the response of $PM_{2.5}$ concentration to precursor emissions varies spatially and temporally, the median and uncertainty are calculated for 171,864 ensembles across the entire modeling domain over 30 days in the episode. We group the results

based on the base $PM_{2.5}$ levels to assess if uncertainties vary with simulated level. Emission-related relative uncertainties for different levels of $PM_{2.5}$ fall into a range from 42% to 52% (Figure 3). This is consistent with the spatial distribution of the relative errors of modeled $PM_{2.5}$ (Figure 4), which shows that most areas have a relative uncertainty in model simulated daily average $PM_{2.5}$ around 40%. Hot spots in the $PM_{2.5}$ concentration field do not have higher relative uncertainties. Instead, the relative uncertainty distributes more evenly over the entire domain, indicating that CMAQ has similar relative uncertainty over a wide range of $PM_{2.5}$ concentrations.

While the daily relative uncertainties calculated here may be high, the uncertainty in the mean PM is likely much lower, though quantifying such would require understanding the temporal and spatial correlations in the emissions uncertainties.

3.3 Comparison with observations

The emission associated uncertainty of simulated $PM_{2.5}$ can be used to investigate how much the difference between the model simulated $PM_{2.5}$ and ground measurements of $PM_{2.5}$ can be explained by emissions uncertainties (Figure 3). The red bars indicate the normalized mean error (NME) between the simulations and available observations of daily $PM_{2.5}$ concentrations fall into various $PM_{2.5}$ levels. The errors between simulated and observed $PM_{2.5}$ are slightly higher than the medians of emissions-associated uncertainties for observed $PM_{2.5}$ concentrations that are between 5 and 15 μg m^{-3}. For observed $PM_{2.5}$ levels that are between 15 and 30 μg m^{-3}, the differences between simulated and observed $PM_{2.5}$ are below the medians of emissions-associated uncertainties. This suggests that the emission-associated uncertainty can explain a large fraction of the simulation errors. Five observation sites in the Houston Ship Channel region were selected for more detailed study (Figure S2). The five sites have available continuous $PM_{2.5}$

monitoring data and a diversity of land use types, which include urban, suburban residential, agricultural, and industrial. They are located to the south, north, and west of the Houston Ship Channel, so they are able to represent various impacts from the areas with intense industrial emissions and as those emissions evolve and are impacted by emissions from other sources, including biogenic.

Modeled and observed daily averages of $PM_{2.5}$ concentrations at the five sites are compared for the entire episode (Figure 5). The error bars represent the emission-associated uncertainties, expressed as the SD (Eq. 3). The dashed lines correspond to the 95% confidence interval (CI), which are obtained by calculating the 2.5th and 97.5th percentiles of the ensemble results. Across the five sites, the percentage of observations that fall in the range of the SD is below 60%, and the percentage of observations that fall in the 95% CI is 85% (Table 3), both slightly less than expected if all of the error were due to uncertainties in the emissions, alone. Both Houston East (AQS#482011034) and Channelview (AQS#482010026) have over 90 percent of the observed concentrations falling in the 95% CI, implying that uncertainties in the emission rates can explain much, but not all, of the difference between the simulated and observed $PM_{2.5}$ concentrations at the two sites (Figures 5a and 5b). The two sites which are south of the Houston Ship Channel (Figures 5c and 5d) have about 70% of the observations in the 95% CI. Modeled $PM_{2.5}$ concentrations are consistently biased high during the last ten days of the episode. These two sites are close to Galveston Bay so the sea breeze can have a large impact on the air pollutant concentrations. The Kingwood site (Figure 5e) exhibits a low bias for $PM_{2.5}$ in the simulation. The reason may be due to its location, which, unlike the other four sites near the Houston Ship Channel, is about 25 miles northeast of Houston's downtown and is located in an area with substantial biogenic VOC emissions. Studies have shown that the current air quality

model tends to underestimate secondary organic aerosols at monitoring sites. Here, the comparison between model simulated and observed concentrations also indicates a low bias. 19 out of 31 monitors had observed daily average $PM_{2.5}$ higher than the upper bound of the standard deviation of the model simulation. This is due in part to the model representation of the chemical reactions, thermodynamic, and the formation of secondary organic aerosols.

During the same period, simulated meteorological fields had higher errors and bias than on the other days: Temperature is biased high in the last ten days of the episode, and wind direction shows larger deviation from observations compared to the first half of the episode. The correlations between the root mean square error of the meteorological fields and that of $PM_{2.5}$ concentrations indicate that the error in $PM_{2.5}$ simulation is related more to errors in wind direction ($R^2 = 0.2$) than to errors in temperature, wind speed, and relative humidity. In addition, the low bias in the $PM_{2.5}$ simulation for August 29-31 at all the five sites is due, in part, to biases associated with meteorological fields. The system simulated a precipitation event occurred from August 29 to 31, which came from north and swept the Houston Ship Channel and the western shore of the Galveston Bay and the heavy rainfall decreased the simulated $PM_{2.5}$ concentration. However, the same reduction is not found in the observed $PM_{2.5}$ concentrations at the five monitoring sites, so the biased-low $PM_{2.5}$ is, in part, attributable to the error in the simulated precipitation and estimated scavenging. The daily precipitation observational data from CPC Unified Gauge-Based Analysis of Daily Precipitation (*http://www.esrl.noaa.gov/psd/cgi-bin/db_search/SearchMenus.pl*) shows that the observed precipitation is located right above the Galveston Bay and moved to the East. The monitors around the Houston Ship Channel were not highly affected by the rain. In contrast, the simulated precipitation is centered at the HGB area, so washout of $PM_{2.5}$ led to low simulated concentrations of $PM_{2.5}$.

316 To further investigate the contribution of uncertain emissions to simulated $PM_{2.5}$, we
317 plotted the histogram of the difference between simulated and observed $PM_{2.5}$ concentrations
318 (i.e., simulated minus observed daily average $PM_{2.5}$ concentrations) at any observation site with
319 continuous $PM_{2.5}$ monitoring data (Figure 6). The probability distribution is close to a log-normal
320 distribution. The mean of the histogram is -1.5 μg m^{-3}, which means the simulated $PM_{2.5}$
321 concentration is generally biased low and is explained by the secondary organic aerosol bias. The
322 standard deviation of the histogram is 8.6 μg m^{-3}, while the average standard deviation of $PM_{2.5}$
323 concentrations due to emissions uncertainties is 7.3 μg m^{-3}. The comparable standard deviations
324 suggest that emission-associated uncertainty can explain a large portion, but not all, of the
325 uncertainty in $PM_{2.5}$ simulations in a regional air quality model.
326
327 3.4 Uncertainties in PM sensitivities
328 Accurately calculating pollutant concentration sensitivities is important because they are
329 directly linked to estimating control strategy effectiveness. The uncertainty of $PM_{2.5}$ sensitivities
330 can be estimated using the same approach of quantifying the emission-associated uncertainty of
331 modeled $PM_{2.5}$. The sampled emissions rates are propagated through the RFM described by Eq. 2
332 for quantification of the emission-associated uncertainty of first order sensitivity of $PM_{2.5}$. The
333 method described by Eq. 3 is applied to calculate the relative uncertainty of the modeled first
334 order sensitivities of $PM_{2.5}$ to the emissions rates of the five major pollutants (i.e., NO_x, primary
335 PM, SO_2, NH_3, and VOC). For each of these sensitivities, their uncertainties are grouped based
336 on the magnitudes of the associated sensitivities, and each group is represented by a bin in the
337 box plot (Figure 7).

In general, the relative uncertainty of each first-order sensitivity decreases when the magnitude of the first-order sensitivity becomes higher. The averages of the median uncertainties for sensitivities of $PM_{2.5}$ to primary PM, NO_x, SO_2, NH_3, and VOC are 16%, 32%, 55%, 75%, and 128%, respectively. These uncertainties are on a relative basis. Taking $\frac{\partial PM_{2.5}}{\partial NO_x}$ for example, its relative uncertainty is 32%, and its simulated value is 1.3 μg m^{-3}, so its standard deviation can be estimated by 32% $\times$ 1.3 μg m^{-3} $\approx$ 0.4 μg m^{-3}, which means its uncertainty on an absolute basis can be expressed as 1.3 ± 0.4 μg m^{-3}. Comparing the five first-order sensitivities, sensitivity of $PM_{2.5}$ to primary PM is the largest one. The spatial average of first-order sensitivity of $PM_{2.5}$ to primary PM on the day of September 8 in the HGB area is 5.2 μg m^{-3}, followed by SO_2 at 1.8 μg m^{-3}, NO_x at 1.3 μg m^{-3}, NH_3 at 0.9 μg m^{-3}, and VOC at 0.8 μg m^{-3}. The standard deviation in the sensitivity caused by uncertainty in emissions rates is comparable (around 1.1 μg m^{-3}) for all species. The same set of perturbations in emissions is applied to each first-order sensitivity, so the magnitude of second-order determines the difference in first-order sensitivities and thus the relative uncertainty. Second-order sensitivities associated with VOC are larger than the others (Table 4). Combined with first-order sensitivity of $PM_{2.5}$ to VOC being the smallest, its relative uncertainty becomes the largest. Second-order sensitivities associated with NO_x are relatively smaller than the others, so the uncertainty of its first order sensitivity is relatively smaller.

Comparison of the uncertainties of the five first-order sensitivities indicates that a first-order sensitivity to a given emission source has less uncertainty associated with emissions if the magnitude of first-order sensitivity is large, i.e., this source has a relatively larger contribution to $PM_{2.5}$ concentration than the other sources, and if first-order sensitivity is much larger (over 10 times in this study) than the magnitudes of its associated second-order sensitivities. This sheds light on whether or not to include certain second-order terms in the RFM: if a second-order

sensitivity has comparable magnitude as its associated first-order sensitivities, it needs to be included in the RFM since it has similar contribution to error propagation as the first-order ones.

4. Conclusions

A reduced form model of CMAQ is applied to propagate the emission uncertainties in Monte Carlo simulations to estimate the related uncertainties in simulated $PM_{2.5}$ concentrations and $PM_{2.5}$ sensitivities. The reduced form model is constructed based on first- and second-order sensitivities obtained from high-order DDM sensitivity analysis in the CMAQ model. The application of the reduced form model saves a substantial amount of computational time (2 - 3 orders of magnitude) in this uncertainty analysis. 1000 possible combinations of emissions rates of five major pollutants are sampled based on a log-normal distribution function with uncertainty factors estimated from a literature search. The ensemble output from the reduced form model is used to quantify the model uncertainty associated with emission rates. The relative uncertainty of modeled 24-hour average of $PM_{2.5}$ concentration is estimated to fall between 42% and 52% for different simulated $PM_{2.5}$ levels. The spatial distribution of the relative uncertainty is fairly uniform over the entire modeling domain.

Comparison of the normalized mean error between simulated and observed $PM_{2.5}$ for different concentration levels suggests that the emission-associated uncertainties can account for a majority of the model error, though the persistent low bias in the summer is attributed to a bias in SOA formation. The time series of simulated and observed daily $PM_{2.5}$ concentrations found that the observations are well captured by model simulation when the emission uncertainties are

383 included. In total, 85% of the measured $PM_{2.5}$ concentrations fall into the 95% confidence
384 interval due to the uncertainty in emission rates and 60 % of the measured $PM_{2.5}$ concentrations
385 fall into the standard deviations. The temporal and spatial trends are well captured in the base
386 simulation. This suggests that much, but not all, of the difference between the observed and
387 simulated concentrations can be attributed to the uncertainty in emission rates. The histogram of
388 errors between simulated and observed $PM_{2.5}$ concentrations has a shape close to a log-normal
389 distribution, with estimated the mean and standard deviation to be -1.5 $\mu g\ m^{-3}$ and 8.6 $\mu g\ m^{-3}$,
390 respectively, and the standard deviation due to uncertain emissions is 7.3 $\mu g\ m^{-3}$, which is
391 comparable to the standard deviation of the model error. While the emissions uncertainties,
392 alone, can explain most of the errors in the model results, other factors, including errors in the
393 meteorological inputs and model parameters, will contribute. We have attempted to minimize
394 the impacts of errors in the meteorological inputs by using detailed meteorological model results
395 that have been thoroughly evaluated well (Angevine et al., 2009, Byun et al., 2011).

396 This paper also demonstrated how to use the RFM approach for estimating the emission-
397 associated uncertainty of sensitivities. Averaged over the HGB area, the emission-associated
398 relative uncertainty of first order sensitivities of $PM_{2.5}$ to primary PM, NO_x, SO_2, NH_3, and VOC
399 emissions are 16%, 32%, 55%, 75%, and 128%, respectively. The first-order sensitivity of $PM_{2.5}$
400 to primary PM emissions is much higher than the other first-order sensitivities, so it has the
401 lowest uncertainty. Uncertainty of a first-order sensitivity to a precursor depends on its
402 associated second-order sensitivities, which determine the magnitude of standard deviation of
403 first-order sensitivity. For example, the first-order sensitivity of $PM_{2.5}$ to VOCs has the largest
404 uncertainty associated with emissions because the VOCs-associated second-order sensitivities
405 have the highest magnitude compared to the others. This indicates that first-order sensitivity has

406 less uncertainty associated with emissions if it is much larger in magnitude (over 10 times in this
407 study) than its associated second-order sensitivities, and that it would be safe to only include this
408 first-order sensitivity in building a RFM which is a function of emission changes.

409 Although the emission-associated uncertainties can explain much of the errors in $PM_{2.5}$
410 simulations, meteorological conditions and model representation of chemical reactions also play
411 an important role. Part of the uncertainty in emissions rates is due to the uncertainty in
412 meteorological fields. In this study, model errors at certain times and locations are associated
413 with relatively high bias in simulated temperature and wind directions. A correlation analysis
414 indicates that the domain-wide model errors in $PM_{2.5}$ simulation is more related to errors in wind
415 direction than to errors in temperature, wind speed, and relative humidity. Besides
416 meteorological conditions, model representation of chemical reactions also contributes to model
417 bias in the $PM_{2.5}$ concentration. The biased-low $PM_{2.5}$ simulation north of Houston suggests that
418 there is a bias in the model representation of the formation of secondary organic aerosol and/or a
419 bias in biogenic VOC emissions in the inventory.
420

Tables

Table 1. Uncertainty factors and associated σ (standard deviations of log-transformed data) of emission rates of five major pollutants.

Emissions	Uncertainty Factor	σ
SO_2	1.62	0.243
NO_x	1.67	0.258
VOC	2.11	0.373
NH_3	2.74	0.505
Primary PM	2.71	0.500

Table 2.Evaluation of WRF-generated meteorological fields from Aug 10 to Sep 14, 2006 with the Techniques Development Laboratory (TDL) surface observations.

	Surface Wind Speed		**Surface Wind Direction**		**Surface Air Temperature**		**Surface Humidity**	
Model Domain Resolution	**Bias ($m\ s^{-1}$)**	**RMSE* ($m\ s^{-1}$)**	**Bias (deg.)**	**Gross Error (deg.)**	**Bias (K)**	**RMSE (K)**	**Bias ($g\ kg^{-1}$)**	**Gross Error ($g\ kg^{-1}$)**
36km	0.23	1.76	2.49	32.78	-0.43	1.96	0.44	0.92
12km	0.53	2.27	14.90	52.08	-0.92	3.34	-0.13	1.18
4km	0.47	1.91	10.50	53.17	0.63	2.29	0.29	1.46

*RMSE: root mean square error

Table 3. Summary of the comparison between simulated and observed daily average $PM_{2.5}$ concentrations.

Site Name	Site Number	Fraction of Days within One Standard Deviation	Fraction of days within 95% CI
Houston East	482011034	83%	93%
Channel View	482010026	69%	97%
Deer Park	482011039	59%	84%
Park Place	482010416	50%	75%
Kingwood	482011042	38%	75%
All Sites		60%	85%

Table 4. First- and second-order sensitivities of $PM_{2.5}$ to emissions. First order sensitivities are calculated as $S_i^{(1)} = \frac{\partial C_{PM_{2.5}}}{\partial E_i}$, second-order self-sensitivities are calculated as $S_{i,i}^{(2)} = \frac{\partial^2 C_{PM_{2.5}}}{\partial E_i^2}$, and second-order cross-sensitivities are calculated as $S_{i,j}^{(2)} = \frac{\partial^2 C_{PM_{2.5}}}{\partial E_i \, \partial E_j}$. E_i and E_j are the i^{th} and j^{th} emissions rates, respectively. The values are daily averages over the HGB area on September 8th, 2006. The unit is μg m^{-3}.

E_i	**First Order**	**Second Order (E_j)**				
		NOx	**PM**	**SO_2**	**NH_3**	**VOC**
NOx	1.3	0.48	0.003	-0.06	-0.002	0.07
PM	5.2		-0.76	-0.37	-0.4	-0.47
SO_2	1.8			-0.76	-0.4	-0.59
NH_3	0.9				-0.88	-0.52
VOC	0.8					-1.16

443 **Figures**

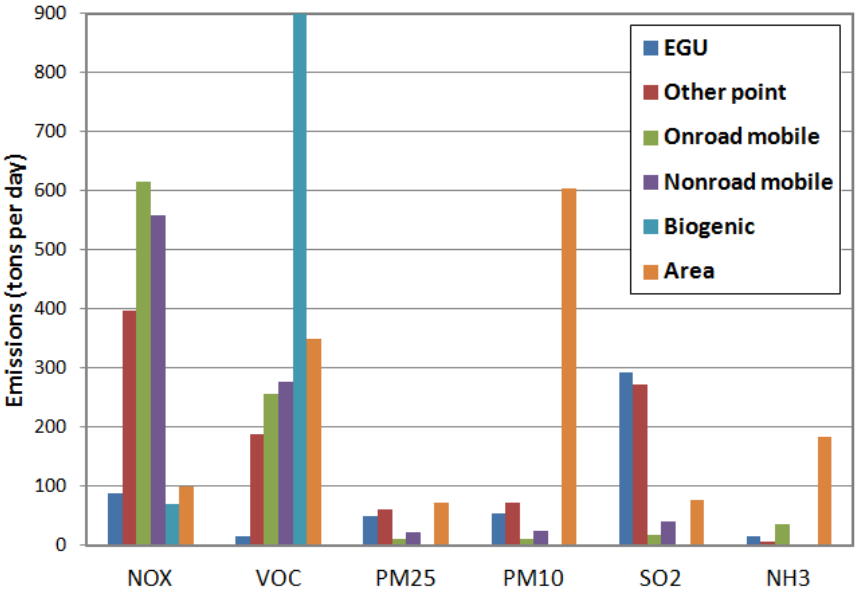

444

445 Figure 1. Emission rates of six major pollutants categorized by emission sources in 2005 NEI.
446 The emission rates are the daily averages of the domain-wide emissions.
447

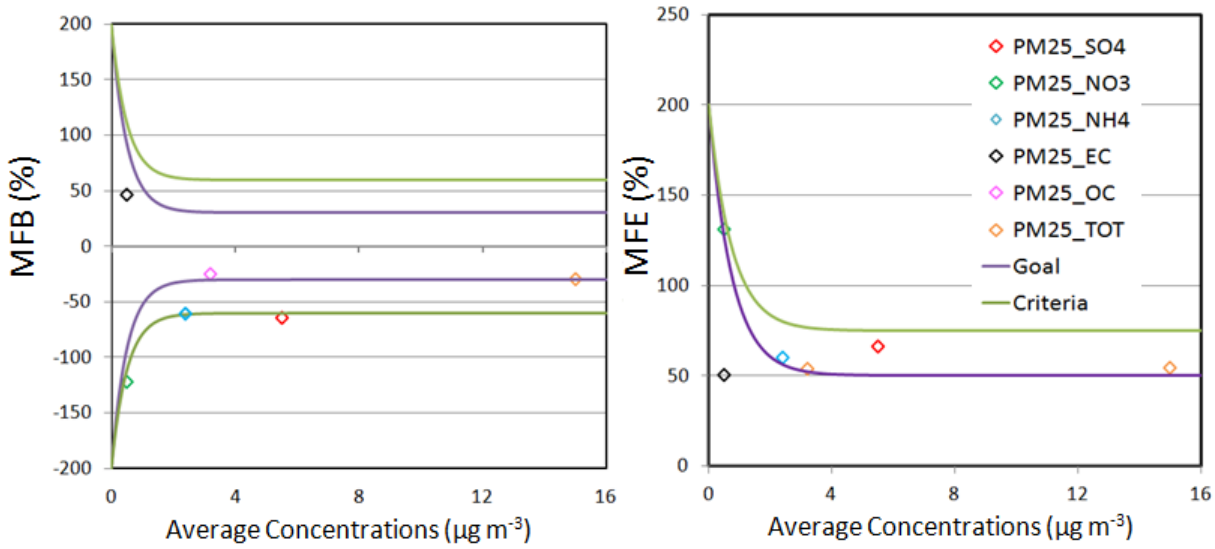

448
449 Figure 2. Bugle plots of CMAQ performance of 24-hour average total and speciation
450 concentrations of $PM_{2.5}$. MFB stands for mean fractional bias and MFE stands for mean
451 fractional error. Goal (purple line) and Criteria (green line) are obtained from Boylan and
452 Russell, 2006. MFB is calculated using $\frac{2}{N}\sum_{i=1}^{N}\frac{C_m-C_o}{C_o+C_m}$, and MFE is calculated using
453 $\frac{2}{N}\sum_{i=1}^{N}\frac{|C_m-C_o|}{C_o+C_m}$, where C_m and C_o are the modeled and observed $PM_{2.5}$ concentrations,
454 respectively. Different markers represent $PM_{2.5}$ and its species, e.g., PM25_TOT means total
455 $PM_{2.5}$, and PM25_SO4 means sulfate aerosol.

456

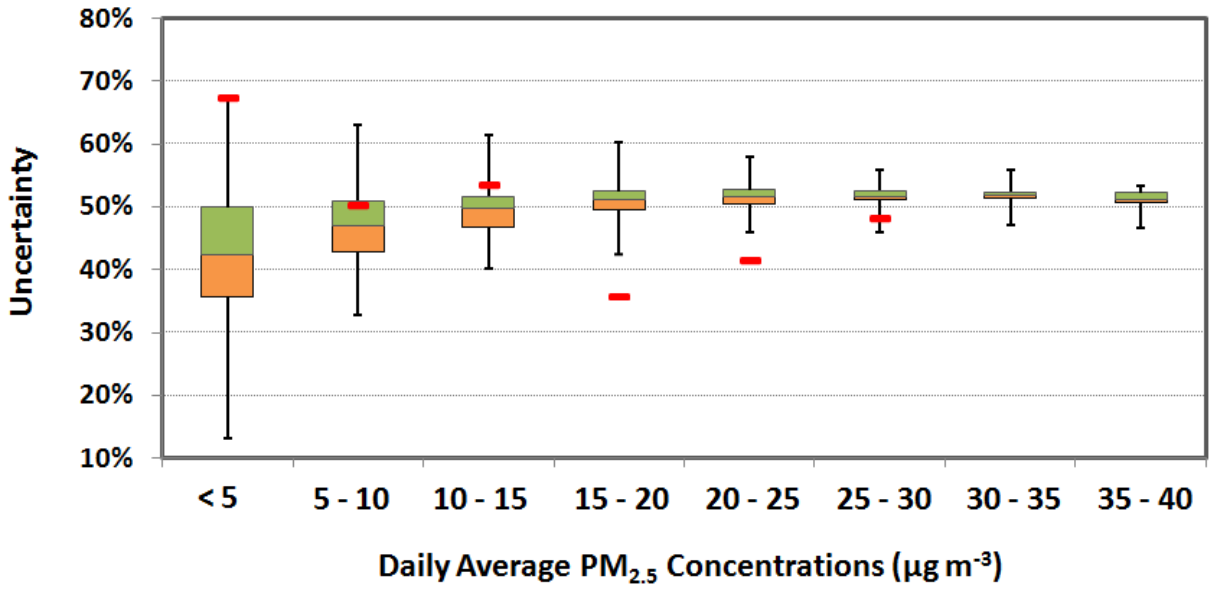

457

458 Figure 3. Relative uncertainty in simulated $PM_{2.5}$ concentrations over the modeling domain. The
459 box shows median, 25th and 75th percentiles. The line between the green and orange boxes
460 represents the median. The whiskers indicate a 95% confidence interval. The red bars indicate
461 the normalized mean errors between observed and simulated $PM_{2.5}$ concentrations at all the
462 observation sites in the modeling domain.
463

a)

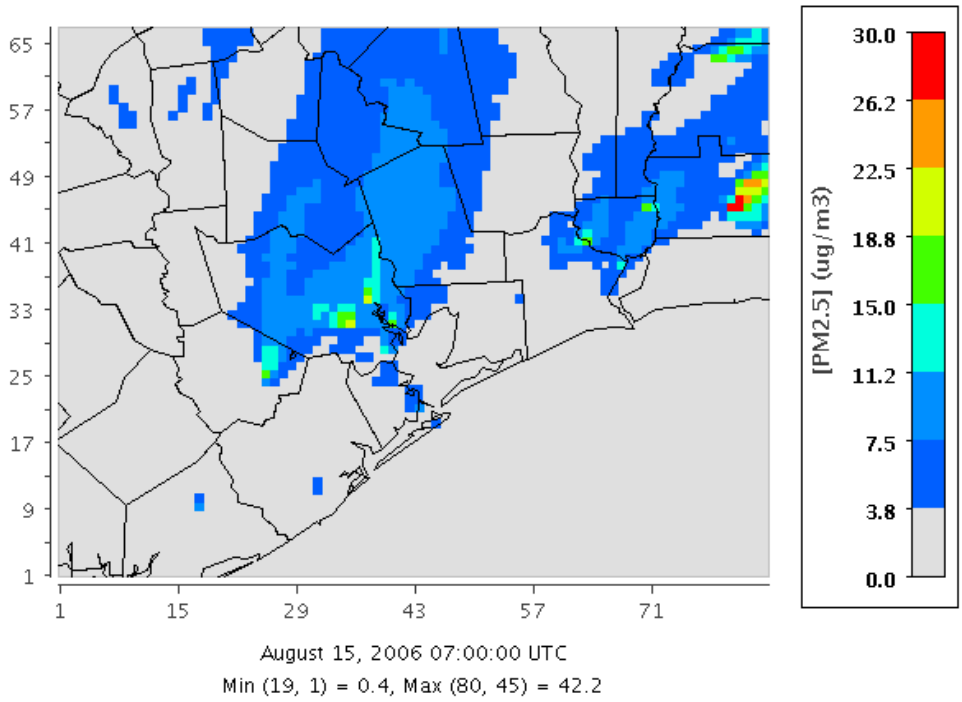

464

b)

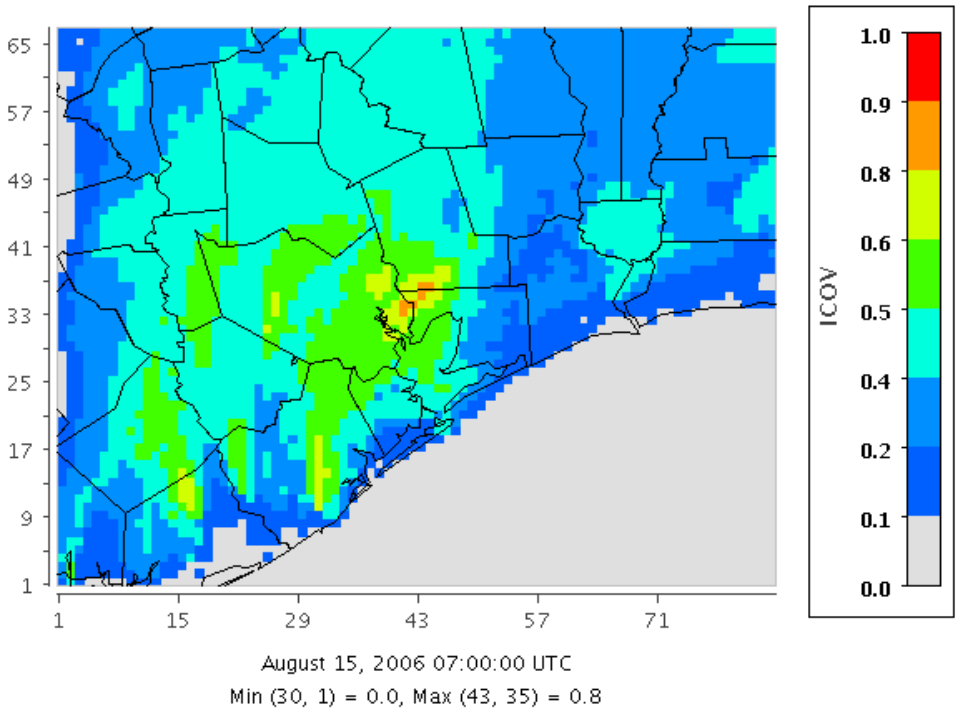

465

466 Figure 4. Spatial distribution of a) daily average $PM_{2.5}$ concentrations and b) uncertainty on
467 August 15, 2006.
468

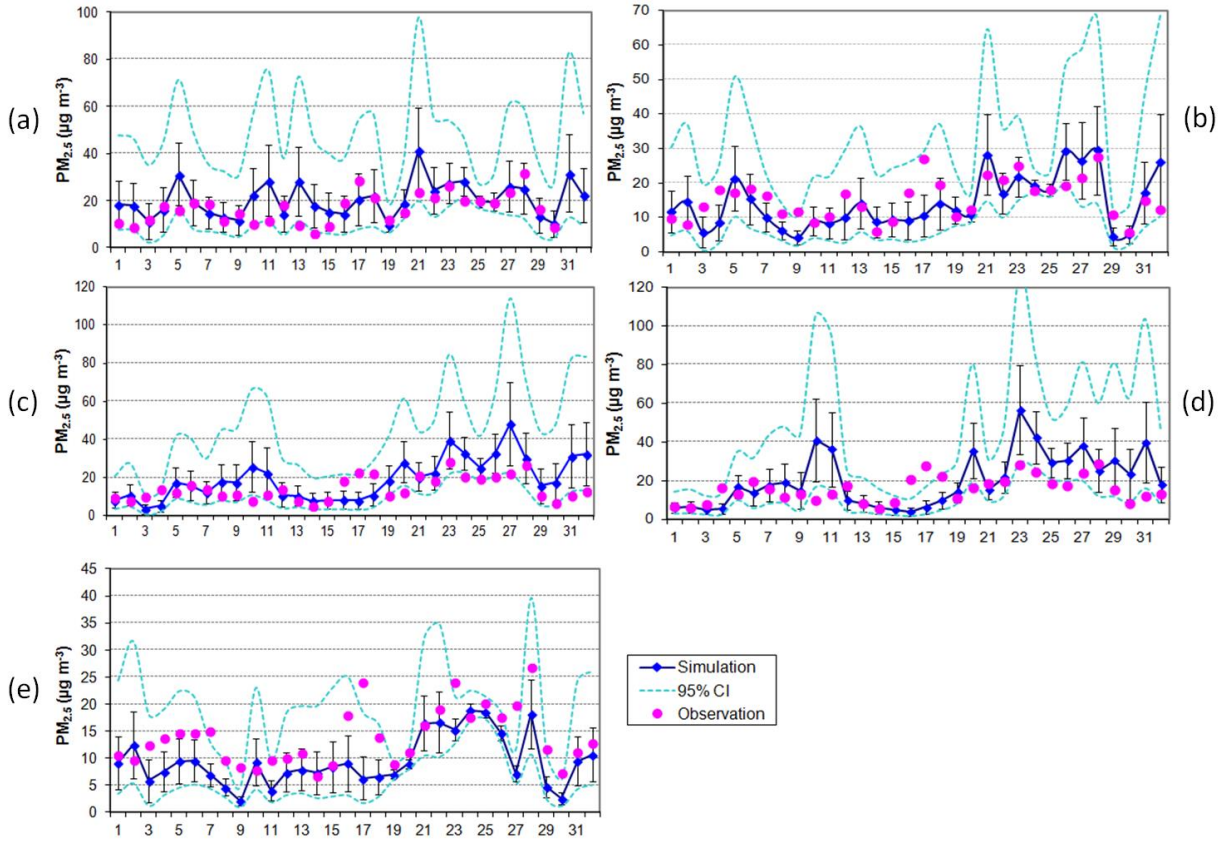

Figure 5. Time series of daily average $PM_{2.5}$ concentrations for the five AQS sites: a) Houston East (AQS#: 482011034), b) Channelview (AQS#: 482010026, c) Deer Park (AQS#: 482011039), d) Park Place (AQS#: 482010416), e) Kingwood (AQS#: 482011042). Blue line with dots stand for simulated $PM_{2.5}$ concentrations; magenta dots stand for observed $PM_{2.5}$ concentrations; light blue dashed line stands for the 95% CI of simulated $PM_{2.5}$ concentrations; error bars correspond to 68.3% CI of $PM_{2.5}$ concentrations, which is equivalent to one standard deviation range.

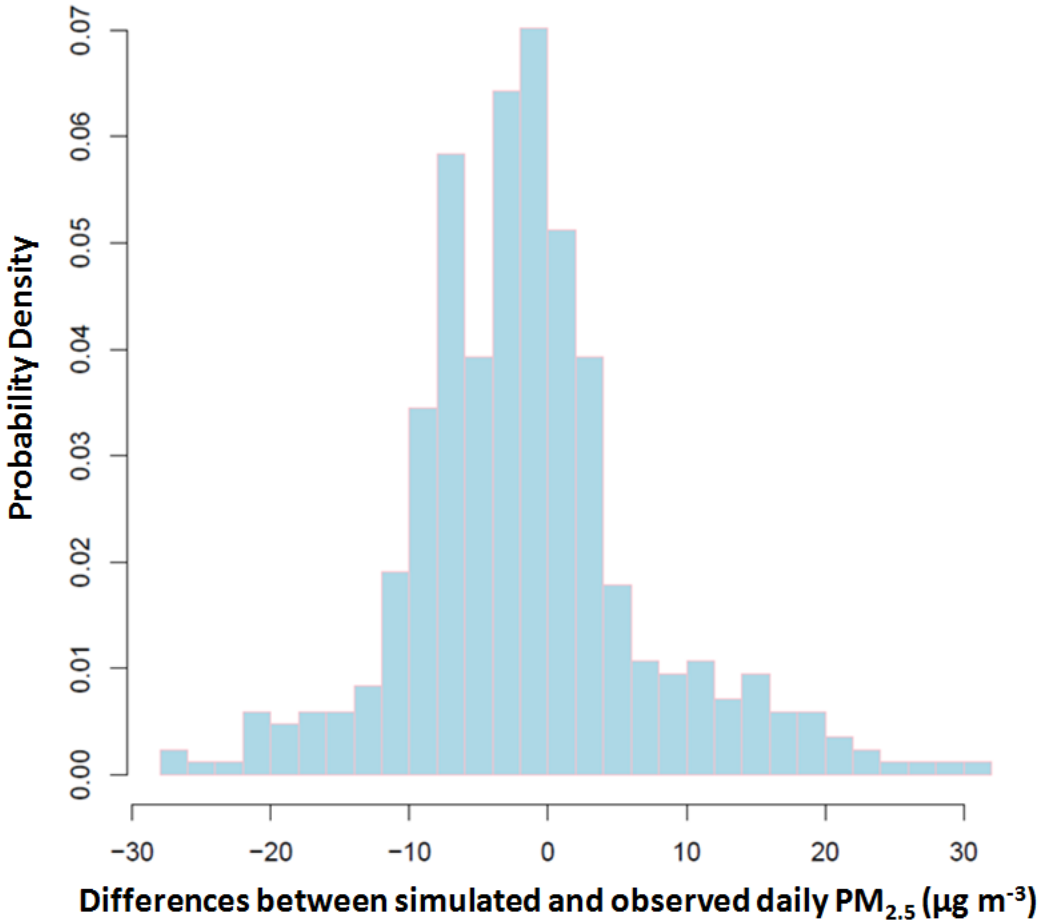

Figure 6. Histogram of differences between CMAQ simulated and observed $PM_{2.5}$ concentrations at all the monitoring sites in the 4km modeling domain.

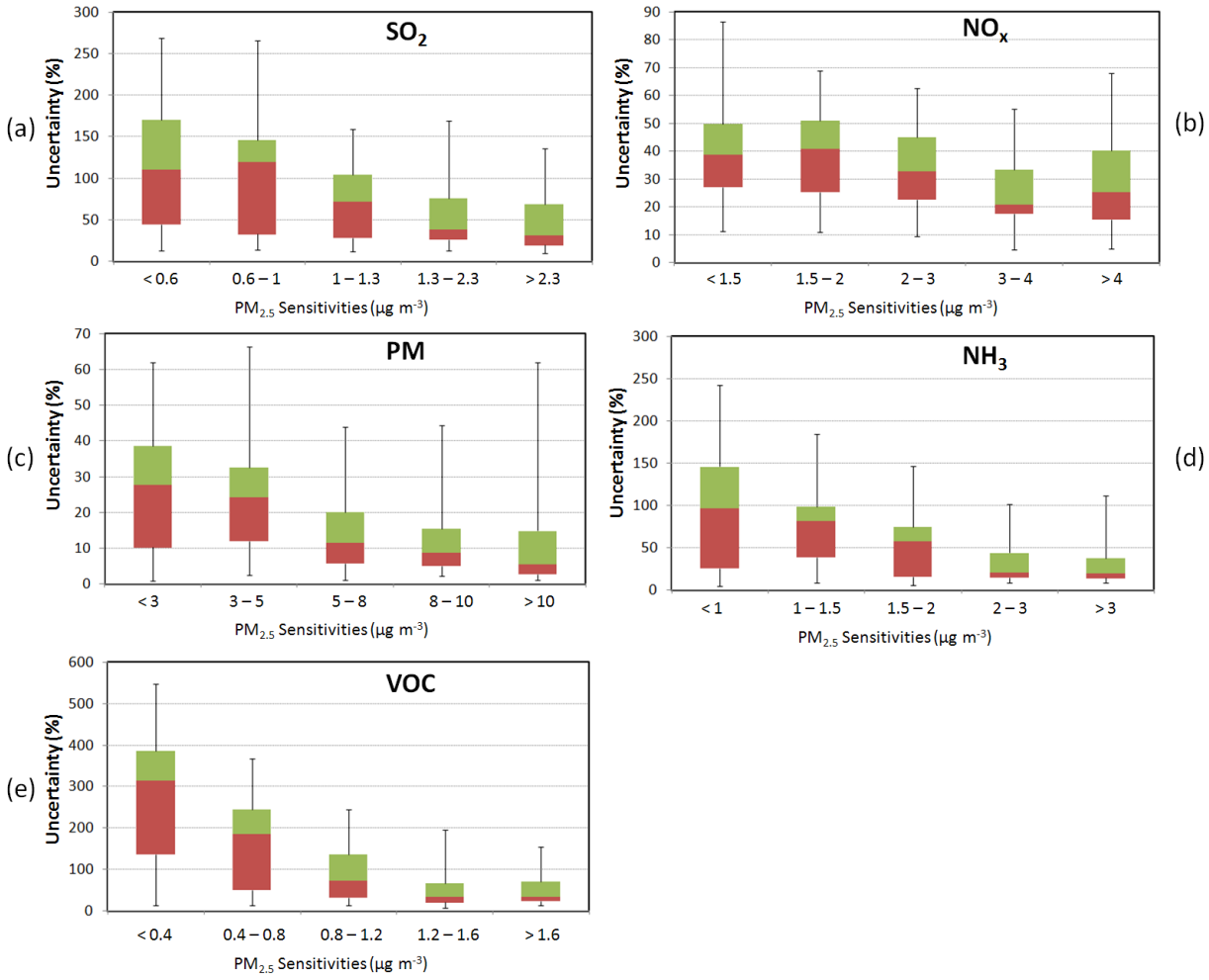

491
492

493 Figure 7. Uncertainty in simulated $PM_{2.5}$ sensitivities due to uncertainties in domain-wide
494 emissions rates of (a) SO_2, (b) NO_x, (c) PM, (d) NH_3, and (e) VOC of the HGB area on
495 September 8, 2007. The box shows median, 25th and 75th percentiles. The line between the green
496 and orange boxes represents the median. The whiskers indicate a 95% confidence interval.

Acknowledgements:

This research was made possible by funding from Phillips 66 Inc., Health Effects Institute, and US EPA STAR grant R834799. While this work was supported, in part, by grant from the US EPA, its contents are solely the responsibility of the grantee and do not necessarily represent the official views of the USEPA. Further, USEPA does not endorse the purchase of any commercial products or services mentioned in the publication. We also acknowledge the contribution of Sergey L. Napelenok of US EPA and Di Tian of Georgia EPD for helpful discussions.

Reference

Angevine, W.M., Zagar, M., Brioude, J., 2009. How well can we model the Houston area for air pollution studies? *Proceedings, Eighth Symposium on the Urban Environment*, January 2009, Phoenix, AZ. http://ams.confex.com/ams/89annual/techprogram/paper_143826.htm.

Banta, R. M., Senff, C. J., Alvarez, R. J., Langford, A. O., Parrish, D. D., Trainer, M. K., White, A. B. (2011). Dependence of daily peak O-3 concentrations near Houston, Texas on environmental factors: Wind speed, temperature, and boundary-layer depth. *Atmospheric Environment*, 45(1), 162-173. doi: 10.1016/j.atmosenv.2010.09.030.

Bergin, M. S., Noblet, G. S., Petrini, K., Dhieux, J. R., Milford, J. B., & Harley, R. A. (1999). Formal uncertainty analysis of a Lagrangian photochemical air pollution model. *Environmental Science & Technology*, *33*(7), 1116-1126. doi: 10.1021/es980749y.

Bergin, M. S., Russell, A. G., Odman, M. T., Cohan, D. S., & Chameldes, W. L. (2008). Single-Source Impact Analysis Using Three-Dimensional Air Quality Models. *Journal of the Air & Waste Management Association*, *58*(10), 1351-1359. doi: 10.3155/1047-3289.58.10.1351.

Boylan, J. W., & Russell, A. G. (2006). PM and light extinction model performance metrics, goals, and criteria for three-dimensional air quality models. *Atmospheric Environment*, *40*(26), 4946-4959. doi: 10.1016/j.atmonsenv.2005.09.087.

Byun, D., & Schere, K. L. (2006). Review of the governing equations, computational algorithms, and other components of the models-3 Community Multiscale Air Quality (CMAQ) modeling system. *Applied Mechanics Reviews*, *59*(1-6), 51-77. doi: 10.1115/1.2128636.

Byun, D., Kim, H., Ngan, F. (2011) Improvement of Meteorological Modeling by Accurate Prediction of Soil Moisture in the Weather Research and Forecasting (WRF) Model. Technical Report submitted to TCEQ, available at https://www.tceq.texas.gov/assets/public/implementation/air/am/contracts/reports/mm/582886246FY1009-NOAA_WRF_Soil_Moisture_20110331.pdf.

Carlton, A. G., Bhave, P. V., Napelenok, S. L., Edney, E. D., Sarwar, G., Pinder, R. W., Houyoux, M. (2010). Model Representation of Secondary Organic Aerosol in CMAQv4.7. *Environmental Science & Technology*, *44*(22), 8553-8560. doi: 10.1021/es100636q

Carter, W.P.L. (2000). Documentation of the SAPRC99 chemical mechanism for VOC and reactivity assessment, Air Pollution Research Center and College of Engineering, Center for Environmental Research and Technology, University of California, Riverside, CA.

Civerolo, K., Hogrefe, C., Zalewsky, E., Hao, W., Sistla, G., Lynn, B., Rosenzweig, C., Kinney, P.L. (2010). Evaluation of an 18-year CMAQ simulation: Seasonal variations and long-term temporal changes in sulfate and nitrate. *Atmospheric Environment*, 44, 6745 – 3752.

Cohan, D. S., Koo, B., & Yarwood, G. (2010). Influence of uncertain reaction rates on ozone sensitivity to emissions. *Atmospheric Environment, 44*(26), 3101-3109. doi: 10.1016/j.atmosenv.2010.05.034.

Cowling, E. B., Furiness, C., Dimitriades, B., Parrish, D., and Estes, M. (2007). Final Rapid Science Synthesis Report: Findings from the Second Texas Air Quality Study, Southern Oxidants Study Office of the Director at North Carolina State University Location: Raleigh, NC, USA

Deguillaume, L., Beekmann, M., and Derognat, C. (2008). Uncertainty evaluation of ozone production and its sensitivity to emission changes over the Ile-de-France region during summer periods. *Journal of Geophysical Research-Atmospheres, 113*(D2). doi: 10.1029/2007jd009081

Digar, A., & Cohan, D. S. (2010). Efficient Characterization of Pollutant-Emission Response under Parametric Uncertainty. *Environmental Science & Technology, 44*(17), 6724-6730. doi: 10.1021/es903743t

Dockery, D. W., Pope, C. A., Xu, X. P., Spengler, J. D., Ware, J. H., Fay, M. E., Speizer, F. E. (1993). An Association Between Air-Pollution and Mortality in Six United-States Cities. *New England Journal of Medicine, 329*(24), 1753-1759. doi: 10.1056/nejm199312093292401.

Emery, et al. (2001) Enhanced meteorological modeling and performance evaluation for two Texas ozone episodes, ENVRION, Novato, CA

ENVIRON. (2005) Users' Guide, Comprehensive Air Quality Model with Extensions (CAMx), Version 4.20; ENVIRON International Corporation.

Foley, K. M., Roselle, S. J., Appel, K. W., Bhave, P. V., Pleim, J. E., Otte, T. L., Bash, J. O. (2010). Incremental testing of the Community Multiscale Air Quality (CMAQ) modeling system version 4.7. *Geoscientific Model Development, 3*(1), 205-226.

570 Galloway, T. S., Brown, R. J., Browne, M. A., Dissanayake, A., Lowe, D., Jones, M. B., and
571 Depledge, M. H. (2004). A multibiomarker approach to environmental assessment.
572 *Environmental Science & Technology, 38*(6), 1723-1731. doi: 10.1021/es030570.

573 Hakami, A., Odman, M. T., & Russell, A. G. (2003). High-order, direct sensitivity analysis of
574 multidimensional air quality models. *Environmental Science & Technology, 37*(11), 2442-
575 2452. doi: 10.1021/es020677h.

576 Hanna, S. R., Chang, J. C., & Fernau, M. E. (1998). Monte Carlo estimates of uncertainties in
577 predictions by a photochemical grid model (UAM-IV) due to uncertainties in input
578 variables. *Atmospheric Environment, 32*(21), 3619-3628. doi: 10.1016/s1352-
579 2310(97)00419-6

580 Hanna, S. R., Lu, Z. G., Frey, H. C., Wheeler, N., Vukovich, J., Arunachalam, S., Hansen, D. A.
581 (2001). Uncertainties in predicted ozone concentrations due to input uncertainties for the
582 UAM-V photochemical grid model applied to the July 1995 OTAG domain. *Atmospheric*
583 *Environment, 35*(5), 891-903. doi: 10.1016/s1352-2310(00)00367-8

584 Hanna, S. R., & Yang, R. X. (2001). Evaluations of mesoscale models' simulations of near-
585 surface winds, temperature gradients, and mixing depths. *Journal of Applied Meteorology,*
586 *40*(6), 1095-1104. doi: 10.1175/1520-0450(2001)040<1095:eommso>2.0.co;2

587 Kaiser, J. (2005). Mounting evidence indicts fine-particle pollution. *Science, 307*(5717), 1858-
588 1861.

589 Kim, S.-W., McKeen, S. A., Frost, G. J., Lee, S.-H., Trainer, M., Richter, A., Angevine, W. M.,
590 Atlas, E., Bianco, L., Boersma, K. F., Brioude, J., Burrows, J. P., de Gouw, J., Fried, A.,
591 Gleason, J., Hilboll, A., Mellqvist, J., Peischl, J., Richter, D., Rivera, C., Ryerson, T.,
592 te Lintel Hekkert, S., Walega, J., Warneke, C., Weibring, P., and Williams, E.: Evaluations
593 of NO_x and highly reactive VOC emission inventories in Texas and their implications for
594 ozone plume simulations during the Texas Air Quality Study 2006, Atmos. Chem. Phys., 11,
595 11361-11386, doi:10.5194/acp-11-11361-2011, 2011.

596 Kwok, R.H.F., Napelenok, S.L., Baker, K.R. (2013). Implementation and evaluation of $PM_{2.5}$
597 source contribution analysis in a photochemical model. Atmospheric Environment, 80, 398
598 – 407.

599 Latha, K. M., & Badarinath, K. V. S. (2005). Shortwave radiative forcing efficiency of urban
600 aerosols - a case study using ground based measurements. *Chemosphere, 58*(2), 217-220.
601 doi: 10.1016/j.chemosphere.2004.09.013.

Lefer, B., Rappengluck, B., Flynn, J., & Haman, C. (2010). Photochemical and meteorological relationships during the Texas-II Radical and Aerosol Measurement Project (TRAMP). *Atmospheric Environment*, 44(33), 4005-4013. doi: 10.1016/j.atmosenv.2010.03.011.

Napelenok, S. L., Cohan, D. S., Hu, Y. T., & Russell, A. G. (2006). Decoupled direct 3D sensitivity analysis for particulate matter (DDM-3D/PM). *Atmospheric Environment, 40*(32), 6112-6121. doi: 10.1016/j.atmosenv.2006.05.039.

Napelenok, S. L., Foley, K. M., Kang, D. W., Mathur, R., Pierce, T., and Rao, S. T. (2011). Dynamic evaluation of regional air quality model's response to emission reductions in the presence of uncertain emission inventories. *Atmospheric Environment, 45*(24), 4091-4098. doi: 10.1016/j.atmosenv.2011.03.030

NARSTO (2004) Particulate Matter Science for Policy Makers: A NARSTO Assessment. P. McMurry, M. Shepherd, and J. Vickery, eds. Cambridge University Press, Cambridge, England. ISBN 0 52 184287 5.

Pinder, R. W., Gilliam, R. C., Appel, K. W., Napelenok, S. L., Foley, K. M., and Gilliland, A. B. (2009). Efficient Probabilistic Estimates of Surface Ozone Concentration Using an Ensemble of Model Configurations and Direct Sensitivity Calculations. *Environmental Science & Technology*, *43*(7), 2388-2393. doi: 10.1021/es8025402.

Ryerson, T. B., Trainer, M., Angevine, W. M., Brock, C. A., Dissly, R. W., Fehsenfeld, F. C., Sueper, D. T. (2003). Effect of petrochemical industrial emissions of reactive alkenes and NO_x on tropospheric ozone formation in Houston, Texas. *Journal of Geophysical Research-Atmospheres*, *108*(D8). doi: 10.1029/2002jd003070

Schwartz, J. (1994). PM_{10}, Ozone, and Hospital Admissions for the Elderly in Minneapolis-Paul, Minnesota. *Archives of Environmental Health, 49*(5), 366-374.

Tian, D., Cohan, D. S., Napelenok, S., Bergin, M., Hu, Y. T., Chang, M., & Russell, A. G. (2010). Uncertainty Analysis of Ozone Formation and Response to Emission Controls Using Higher-Order Sensitivities. *Journal of the Air & Waste Management Association, 60*(7), 797-804. doi: 10.3155/1047-3289.60.7.797.

U.S. EPA (2004) Air quality criteria for particulate matter. EPA/600/P-99/002aF.

U.S. EPA. (2007). Guidance on the Use of Models and Other Analyses for Demonstrating Attainment of Air Quality Goals for Ozone, $PM_{2.5}$, and Regional Haze. *EPA -454/B-07-002*.

Xiao, X., Cohan, D. S., Byun, D. W., & Ngan, F. (2010). Highly nonlinear ozone formation in the Houston region and implications for emission controls. *Journal of Geophysical Research-Atmospheres, 115*. doi: 10.1029/2010jd014435.

Watson, J. G. (2002). Visibility: Science and regulation. *Journal of the Air & Waste Management Association, 52*(6), 628-713.

Wert, B. P., Trainer, M., Fried, A., Ryerson, T. B., Henry, B., Potter, W., Wisthaler, A. (2003). Signatures of terminal alkene oxidation in airborne formaldehyde measurements during TexAQS 2000. *Journal of Geophysical Research-Atmospheres, 108*(D3). doi: 10.1029/2002jd002502.

Yang, Y. J., J. G. Wilkinson, and A. G. Russell (1997) Fast, direct sensitivity analysis of multidimensional photochemical models. Environmental Science & Technology, 31, 2859-2868.

Yu, S, Dennis, R, Roselle, S., Nenes, A., Walker, J., Eder, B., Schere, K., Swall, J. and Robarge, W. (2005). An assessment of the ability of three-dimensional air quality mode with current thermodynamic equilibrium models to predict aerosol NO3. *Journal of Geophysical Research*, 110, D07S13, doi:10.1029/2004JD004718.

Zanobetti, A., Schwartz, J., and Dockery, D. W. (2000). Airborne particles are a risk factor for hospital admissions for heart and lung disease. *Environmental Health Perspectives, 108*(11), 1071-1077. doi: 10.1289/ehp.001081071.

Zhang, W., Capps, S. L., Hu, Y., Nenes, A., Napelenok, S. L., and Russell, A. G. (2012). Development of the high-order decoupled direct method in three dimensions for particulate matter: enabling advanced sensitivity analysis in air quality models. *Geoscientific Model Development, 5*(2), 355-368. doi: 10.5194/gmd-5-355-2012

Zhang, Y., Vijayaraghavan, K., Wen, X., Snell, H.E., and Jacobson, M.Z. (2009). Probing into regional ozone and particulate matter pollution in the United States: 1. A 1 year CMAQ simulation and evaluation using surface and satellite data. *Journal of Geophysical Research*, 114, D22304, doi:10.1029/2009JD011898.